

# Slow relaxation of spinless fermions with long-range Coulomb interactions on one dimensional lattices

Zhi-Hua Li

*School of Science, Xi'an Technological University, Xi'an 710021, China*

We study transport and relaxation of spinless fermions with long-range Coulomb interactions by out of equilibrium dynamics. We find the relaxation is continuously slowing down with stronger coupling  $V$  and there is a transition in the transport type. For intermediate  $V$ , the system displays normal diffusive transport, however the relaxation time is long and scales with  $V$  in power laws. For large  $V$ , the relaxation time diverges exponentially with system lengths, featuring a MBL-like phase, while at the same time it supports subdiffusion transport. We attribute the slow relaxation to possible bound states, which become slower with increasing  $V$ .

## I. INTRODUCTION

Understanding how macroscopic hydrodynamics is emerged from microscopic laws is an important question, which is in general difficult to answer. However, in recent years a breakthrough has been made for integrable systems, which is coined generalized hydrodynamics (GHD)[1, 2]. It has been established in GHD that integrable systems can support ballistic transport at finite temperatures due to existence of infinite many conserved charges. Various transport quantities for many 1D quantum integrable models have been calculated [3]. In particular, it has been applied to XXZ model for its ballistic[4], diffusion [5] and superdiffusion [6, 7] regimes.

Although GHD is successful for integrable systems, integrability is rare in the real world and there are always various perturbations to break it. On the one hand, some groups have attempted to incorporate (weak) integrability breaking terms into GHD [8, 9]. On the other hand, transport of many non-integrable models have been studied numerically. These include the XXZ model with dimerization and frustration [10], staggered field [11], and spin ladders [12, 13], just to name a few. Although in majority cases transport would become diffusive, as is expected, there are other cases transport are anomalous [5, 11]. Our understandings of transport of non-integrable models are still far from complete.

In previous studies the integrability breaking terms are mostly short-ranged, in which the relaxation processes are usually short and the systems retain diffusive in large coupling limit. In this paper, we study transport and relaxation of a fermion model with translation invariant long-range interactions on 1D lattices (1). We found that the transport and relaxation is continuously slowing down with stronger coupling  $V$ , and there is even a transition of transport type. We demonstrate these by studying two quantities  $z(t)$  and  $f(t)$ , both of which are extracted from out of equilibrium dynamics: the former is from a bipartite quench protocol, while the later is from evolution of initial states with random classical configurations. For intermediate  $V$ , both  $z$  and  $f$  would reach their thermalized values, however, each of them relaxes slowly in a logarithmic manner and the relaxation time

scales with  $V$  in power laws. For large  $V$ , the relaxation time for  $f$  diverges with system sizes  $\sim e^{\sigma L}$ , at the same time,  $z$  is kept finite below 0.5, implying a subdiffusion transport.

We argue that there may exist slow bound states which cause slow relaxation. For a generic quantum lattice model with a limited band width  $\sim \lambda$ , bound states composed with  $n$  particles could form. When  $V \gtrsim \lambda$ , the group velocity of the bound state should be exponentially slow in  $n$ . Besides, we find that faster particles are always backscattered by the long-range interactions. Hence the slow bound states behave as barriers for the faster ones, which slow down the relaxation process. At large coupling  $V \gg \lambda$ , the bound states move so slow that they resemble static disordered potentials in the context of many body localization (MBL), then a transition to MBL-like state occurs.

Several papers have already discovered MBL-like phase in disorder-free models [14–20]. Those works usually introduced fast and slow particles manually. While we take the point of view that slow particles can be self-generated bound states, which was pioneered by Kagan and Maksimov [14]. This is more natural and closer to realizable physical systems such as carbon nanotube or cold atom systems [21, 22]. In addition, there has been ambiguity about the nature of the quasi-MBL state [23]. We elucidate that the quasi-MBL state can be coincided with subdiffusion transport (at least for the present model).

## II. MODEL

The model considered here consists of a chain with  $L$  sites,

$$\begin{aligned} \hat{H} = & -\lambda \sum_i (\hat{c}_i^\dagger \hat{c}_{i+1} + h.c.) \\ & + \sum_{i < j} \frac{V}{|j - i|^\alpha} (\hat{n}_i - 1/2)(\hat{n}_j - 1/2) \end{aligned} \quad (1)$$

where  $\hat{c}_i^\dagger$  ( $\hat{c}_i$ ) is creation (annihilation) operator of a spinless fermion, and  $\hat{n}_i$  is a fermion density operator at site  $i$ . The interaction decays in power law governed by an

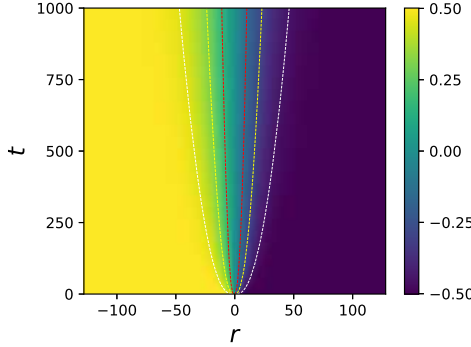


FIG. 1. Time evolution of scaled spin density  $\mu^{-1}m(r, t)$  at  $V = 4$  for a chain of  $L = 256$  sites. The origin for the  $r$  axis is shifted to  $L/2$ . Dashed are contour lines.

exponent  $\alpha$ . Its ground state properties have been studied in [24–27]. Here we investigate its transport and dynamics at high temperatures. We fix  $\alpha = 1$  which corresponds to unscreened Coulomb potential, and use the unit  $\lambda = \hbar = 1$  throughout the paper.

This model can be rewritten via the Jordan-Wigner transformation as a quantum spin model with long-range coupling in the  $z$  component. In particular, at  $\alpha = \infty$ , it reduces to the XXZ model with the exchange coupling  $J = |2\lambda| = 2$  and anisotropy  $\Delta = V/2$ . By virtue of this, we use the languages for fermion and spin systems interchangeably, and rephrase charge transport as spin transport. The total magnetization  $M = \sum_i \hat{S}_i^z$  is conserved. When there is inhomogeneity of spin density, spin is transported, so that the system might eventually relax to equilibrium state. The spin transport can be measured through the current operator  $\hat{j}_i = J(\hat{S}_i^x \hat{S}_{i+1}^y - \hat{S}_i^y \hat{S}_{i+1}^x)$ . We study transport and relaxation dynamics of model (1) as a function of  $V$ , for  $V \gtrsim 2$ , where slow bound states could form.

### III. DYNAMICAL EXPONENT FROM A BIPARTITE QUENCH PROTOCOL

We use a dynamical exponent extracted from a quench dynamics to characterize transport. The initial states for the quench dynamics are mixed type domain-wall states [28],

$$\rho(t=0) \sim (1 + \mu\sigma^z)^{\otimes \frac{L}{2}} \otimes (1 - \mu\sigma^z)^{\otimes \frac{L}{2}}, \quad (2)$$

where  $\mu$  induces an imbalance of magnetization in the system: magnetization of the left (right) half of the system is  $+\frac{1}{2}\mu$  ( $-\frac{1}{2}\mu$ ).  $\mu$  will be set to 0.01, that is the system is weakly-polarized and can be understood as in high temperature state [28]. We numerically integrate the quantum Leibniz equation to obtain  $\rho(t)$  using a two-site version of the time dependent variation principle algorithm (TDVP) [29]. This algorithm can deal

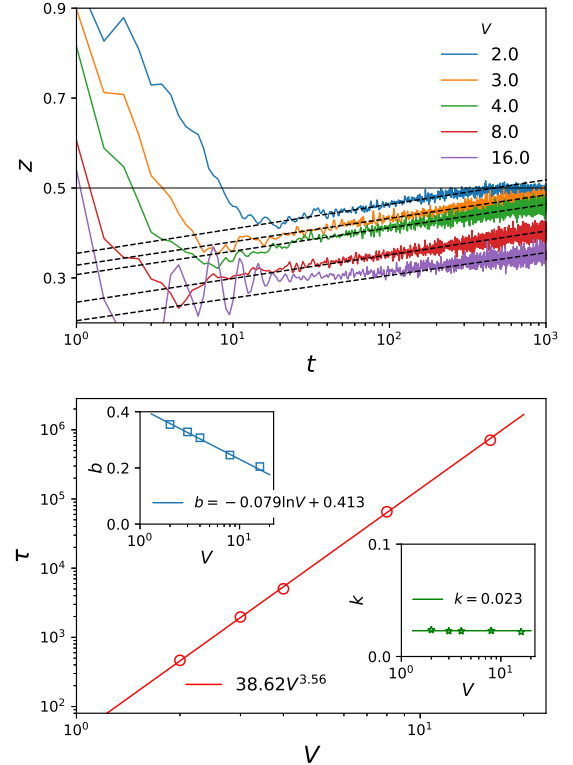


FIG. 2. Upper panel: dependence of dynamical exponent  $z$  on time, which is expected to eventually reach 0.5 (horizontal solid line) for each coupling strength  $V$ . Dashed are fittings to (5). Lower panel: relaxation time  $\tau$  (and the fitting parameters  $b$  and  $k$ , in the two inset panels) as a function of  $V$ . The values of  $\tau$  are determined through (6). Symbols are data, while solid lines are fitting functions as indicated in the legends.

with Hamiltonians with long-range interactions through a matrix product operator (MPO) technique [30].

Once  $\rho(t)$  is obtained, the transport property can be extracted by the profiles of magnetization  $m(r, t) = \text{tr}[\rho(t)\hat{S}_r^z]$  or by the current  $j_r(t) = \text{tr}[\rho(t)\hat{j}_r]$ . An example of  $m(r, t)$  is shown in Fig. 1. One expects that, at large time, it will have a scaling form  $m(r, t) = f(\xi)$ , with the scaling variable  $\xi = (r - L/2)/t^z$ . Then the type of transport can be determined by the exponent  $z$ : it is ballistic if  $z = 1$ , diffusive if  $z = 0.5$  and subdiffusive if  $z < 0.5$ .

In practice  $z$  is time dependent before reaching its asymptotic value. We extract  $z$  alternatively by measuring accumulation of spins transported through center of the chain

$$\Delta m(t) \equiv \int_0^t j_{\frac{L}{2}}(t') dt' \propto t^z \quad (3)$$

Then the time dependence can be obtained conveniently through

$$z(t) = d \ln(\Delta m) / d \ln(t). \quad (4)$$

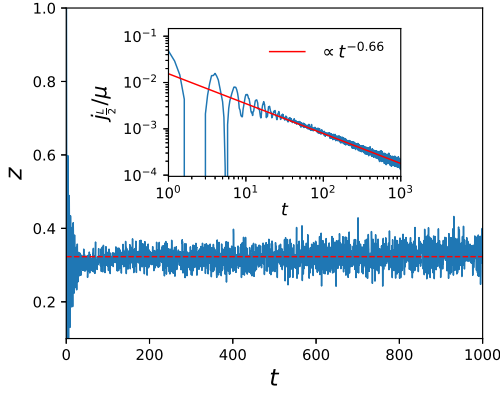


FIG. 3. Time dependence of dynamical exponent at  $V = 32$ . The exponent oscillates around  $z = 0.32$  (red dashed line) at late times. Inset panel shows current flowing through center of the lattice, which decays in power law at late times (red solid line).

Fig.2 shows  $z(t)$  for intermediate coupling strengths. It appears that  $z$  will reach 0.5 for each  $V$  at large time, which indicates the transport is eventually diffusive. However, before that  $z$  increases slowly and the late time dynamics can be fitted by a logarithmic function

$$z(t) = k \ln(t) + b, \quad (5)$$

The fitting parameters  $k$  and  $b$  may depend on  $V$ . Thanks to this relation, one can estimate a relaxation time  $\tau$  for when  $z$  reaches the thermalized value of 0.5, which would be otherwise difficult to reach in simulation. Namely, it is determined by the fitting parameters,

$$\tau = e^{(0.5-b)/k} \quad (6)$$

The lower panel shows dependence of  $\tau$  (and also  $b$  and  $k$ , in the two inset panels) on  $V$ .  $\tau$  increases with  $V$  in a power law

$$\tau \propto V^\kappa, \quad (7)$$

with an exponent  $\kappa \simeq 3.56$ .  $b$  decreases with  $V$  which can be fitted in the form  $b(V) = A \ln V + B$ , while  $k$  seems to be a constant. So the dependence of  $\tau$  on  $V$  is solely coming from that of  $b$  on  $V$ . These lead to a refined form for (5) as  $z(t) = k \ln(t) + A \ln V + B$ , with the constant coefficients  $k = 0.023$ ,  $A = -0.079$  and  $B = 0.413$ .

In the above we have shown that, even if the system retains diffusion transport, the transport and relaxation is slowed down upon tuning coupling to stronger values. In fact the above relations (5) and (7) may hold only for intermediate range of couplings. For large couplings, say  $V = 32$ ,  $z$  keeps vibrating around a constant value at late times that is below 0.5 (see Fig.3). This indicates that transport is even slowed at large  $V$  and a transition to subdiffusion occurs.

Note that the above relaxation time and other quantities, drawn from the bipartite quench, are essentially

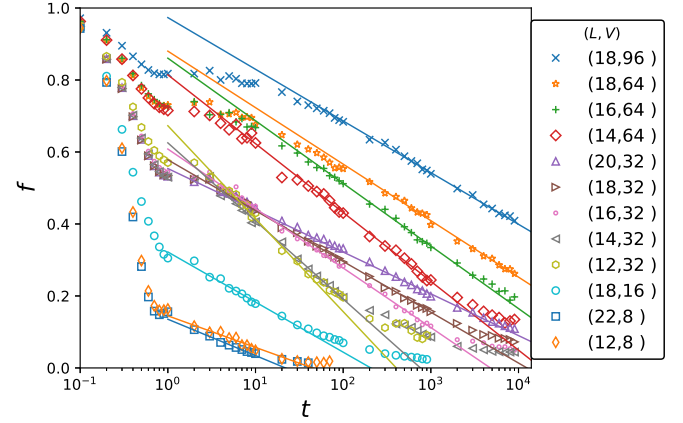


FIG. 4. Relaxation process of spatial density inhomogeneity for pairs of different couplings and system sizes. Solid lines are fittings to a logarithmic function (10).

thermodynamic limit values. Next we corroborate the above observations by studying dynamics for short finite systems but longer time scales.

#### IV. RELAXATION FROM SPATIAL DENSITY INHOMOGENEITY

We use the dynamics of spatial inhomogeneity of particle density as a measure of relaxation process. It is defined by [18]

$$\Delta\rho_\psi^2(t) = \frac{1}{L} \sum_{i=1}^L [\langle \psi(t) | \hat{n}_{i+1}(t) - \hat{n}_i(t) | \psi(t) \rangle]^2 \quad (8)$$

Classical configurations such as  $|\psi\rangle = |01001 \cdots 010\rangle$  are used as initial states, then they are evolved under (1) with periodical boundary conditions through an exact diagonalization algorithm [31]. An average value  $\langle \Delta\rho_\psi^2(t) \rangle$  is taken for  $\psi$  drawn from sectors with fixed filling factor  $\nu$  (number of particles divided by  $L$ ) and is divided by its initial value, which defines a quantity

$$f(t) \equiv \frac{\langle \Delta\rho_\psi^2(t) \rangle}{\langle \Delta\rho_\psi^2(0) \rangle}. \quad (9)$$

This quantity should remain finite for infinite time, if the system is localized, otherwise it thermalizes. Each data of  $f$  shown below are obtained by using 300 realizations of  $\psi$  at  $\nu = \frac{1}{2}$ .

Fig.4 shows relaxation of  $f$ , for  $t$  up to  $10^4$  for several  $(L, V)$  pairs in the ranges  $12 \leq L \leq 22$  and  $8 \leq V \leq 96$ .  $f$  clearly reaches 0 for small  $L$  and  $V$ , while decays slower for larger  $L$  and  $V$ . It is expected that the relaxation time  $\tau_1$ , defined as  $f(\tau_1) = 0$ , are finite for large (but finite)  $L$  and  $V$  as well. There are multiple time scales before thermalization, a notorious one being the logarithmic process

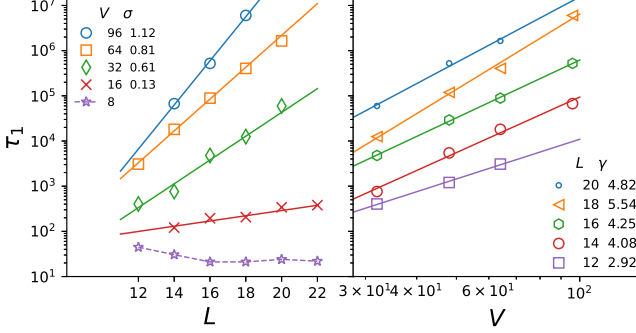


FIG. 5. Left panel: dependence of relaxation time on system sizes with fixed couplings. Solid lines are fittings to (12) with the exponents  $\sigma$  shown in the legend. Dashed line is guide for the eye. Right panel: dependence of relaxation time on coupling strengths with fixed lattice lengths. Lines are fittings to (13).

at late times, which can be fitted nicely with functions of the form

$$f(t) = -k_1 \ln t + b_1. \quad (10)$$

Here the fitting parameters  $k_1$  and  $b_1$  would depend on  $(L, V)$ . We use (10) to estimate the relaxation time by

$$\tau_1 = e^{b_1/k_1}. \quad (11)$$

The left panel of Fig.5 shows dependences of  $\tau_1$  on  $L$  with fixed couplings. For small  $V$ ,  $\tau_1$  saturates with increasing  $L$ , which means the system thermalizes in thermodynamic limit. Whereas, for each large  $V$ ,  $\tau_1$  grows exponentially with  $L$ ,

$$\tau_1 \propto e^{\sigma L}, \quad (12)$$

with an exponent  $\sigma$  possibly depends on  $V$ . This relation means lack of thermalization and corresponds to a quasi-MBL phase introduced in [19]. So there is a transition between small and large coupling regimes, however, we are not meant to locate a transition point  $V_c$  precisely in this paper. The right panel shows dependence of  $\tau_1$  on  $V$  in the large  $V$  regime. For each system sizes,  $\tau_1$  grows with  $V$  in a power law,

$$\tau_1 \propto V^\gamma, \quad (13)$$

with an exponent  $\gamma$  possibly depending  $L$ .

It is tempting to obtain a full function relation  $\tau_1(L, V)$  for large  $V$ . (12) and (13) alone are not sufficient. We can obtain it by utilizing the dependence of  $b_1$  and  $k_1$  on  $(L, V)$ , as shown in Fig.6. For fixed  $L = 18$  (left panel),  $k_1$  clearly does not depend on  $V$ ; while  $b_1$  increases logarithmically with  $V$ , which can be fitted with the form  $b_1 = C \ln V + D$ . So the power law of (13) is actually coming from the logarithmic dependence of  $b_1$  on  $V$ . Next, for a fixed  $V = 32$  (right panel),  $k_1$  reduces

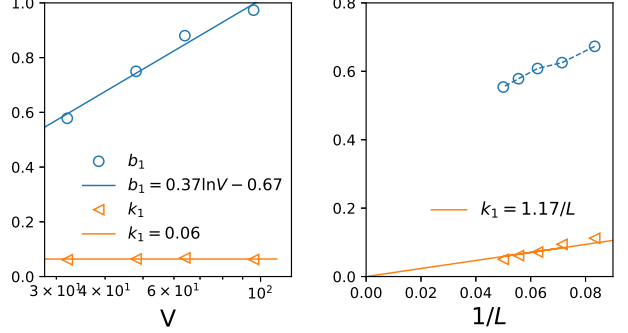


FIG. 6. Dependence of fitting parameters  $b_1$  and  $k_1$  on coupling strengths for fixed  $L = 18$  (left panel) and inverse system lengths at fixed  $V = 32$  (right panel), respectively. Solid lines are fitting functions, as indicated in the legend. Dashed line is guide for the eye.

with system lengths as  $k_1 = u/L$ . The above analysis implies a refined form of (10)

$$f(t) = -\frac{u}{L} \ln(t) + C \ln V + D. \quad (14)$$

and that

$$\tau_1(L, V) = e^{(C \ln V + D)L/u} \quad (15)$$

in the regime  $V > V_c$ . The factor  $u$  must be a constant, as  $k_1$  depends solely on  $L$ . In thermodynamic limit  $k_1 \rightarrow 0$  and  $f(t \rightarrow \infty) = b_1 > 0$ , the system is asymptotically localized [For  $V < V_c$ , one may replace  $u/L$  with a finite constant, so that  $f(t) = 0$  for  $t \geq \tau_1$  in thermodynamic limit].  $b_1$  depends on both  $(L, V)$ , with the  $L$  dependence contained in the coefficients  $C$  and  $D$ . To make (15) consistent with (12), the only possibility is  $C(L) = \text{const.} + E/L + \mathcal{O}(1/L^2)$ .  $D(L)$  should also have a similar form for the same reason. At large  $L$ ,  $C$  and  $D$  can be approximately taken as constants. We use this approximation and plot the  $u/L$ -th root of  $\tau_1$  versus  $V$  in Fig.7. The nearly collapse of data (especially for larger  $L$ ) indicates that (15) is plausible.

## V. ROLES OF BOUND STATES

For quantum integrable systems the existence of bound states as quasi-particles is well established [32, 33]. The success of GHD just relies on identifying those quasi-particles as charge carriers. In particular for the XXZ model, a bound state is referred to as a  $n$ -string, which corresponds to a sequence of  $n$  flipped spins (with the 1-string reducing to a single magnon). It has a group velocity  $\sim \Delta^{-(n-1)}$  [34] and scatters forwardly with one another. Note that at large  $\Delta$  and  $n$ , its velocity is so slow that it resembles a sequence of  $n$  localized spin block [35].

For generic quantum lattice models bound states should also exist, which does not rely on integrability, but

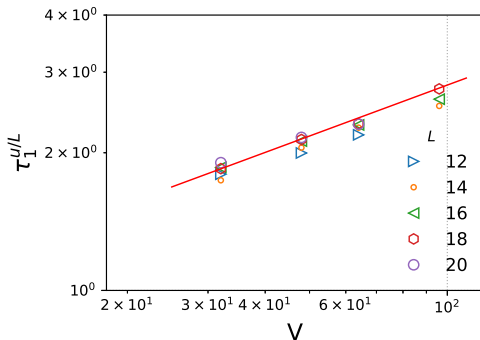


FIG. 7. Rescaled relaxation time vs. coupling strength with different system sizes. The  $y$ -axis is  $u/L$ -th power of  $\tau_1$ , with  $u = 1.17$ . The solid line is  $e^{C \ln V + D}$ , with  $C = 0.37$  and  $D = -0.67$ . Nearly collapse of the data to this line for each  $L$  validates (15).

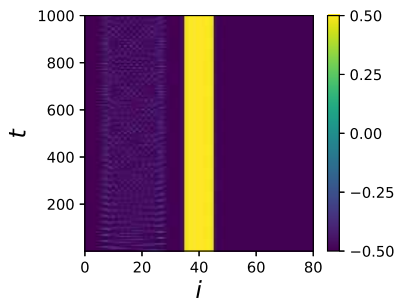


FIG. 8. Collision of a Gaussian wave packet like magnon with a block of 10 localized spins at  $V = 8$ . The color map shows density of spins. The magnon is backscattered back and forth between the left boundary and the spin block.

on limited band widths. And they are expected to play an essential role in transport likewise. For  $n = 2$  particles, this can be proven for general interaction potentials, no matter it is attractive or repulsive [14, 36, 37]. For  $n > 2$  particles, there still lacks a general theory [14, 38, 39]. However, their existence may be anticipated from a simple energy conservation perspective: when the potential energy of a compact  $n$  particle cluster is much greater than the bind width, it can't decay into smaller spatially separated pieces, hence the cluster is close to an eigenstate. These arguments also applies for the long-range model (1). There should be  $n$  particle bound states, with an effective hopping  $\sim V^{-(n-1)}$  in  $n^{\text{th}}$  order of perturbation theory.

Transport and relaxation not only depend on the content of bound states but also on their collision properties. We use a simulation of few spin dynamics that has been applied to integrable models [40, 41] to investigate that. Specifically, we collide a Gaussian wave packet like magnon (see appendix A for details of its definition) and a localized spin block, as plotted in Fig.8. The spin block is stable for long time, which implies that it is close to

an eigenstate of the Hamiltonian and resembles a slow moving  $n$  particle bound state. Then one can see the light magnon is always backscattered by the spin block (the approximate bound state).

Existence of slow bound states and pure reflective scattering should be the cause for slowing down of transport and relaxation. With growing  $V$ , the only mobile modes are the magnons, moving in the background of slow bound states, then the system fails to thermalize when  $V$  exceeds some threshold.

## VI. CONCLUSION

We studied finite temperature transport and relaxation of the fermion model with long-range Coulomb potential in a wide range of couplings. We simulated two quantities  $z(t)$  and  $f(t)$ , which are complementary: the former is for large system lengths, shorter time and smaller  $V$ , while the later is more suitable for small  $L$ , longer time and larger  $V$ . The results are overall consistent: both  $z$  and  $f$  decays with time in logarithmic functions; both relaxation times  $\tau$  and  $\tau_1$  scales with  $V$  in power laws for all ranges of  $V$  when  $L$  is finite, while diverges for large  $V$  when  $L$  is infinite. All these together showing slowing down of relaxation with increasing  $V$ , besides an identification of the quasi-MLB phase with a subdiffusion transport.

The slow relaxation is caused by both slow bound states and complete backscattering of light particles. It may be found in a wide range of generic non-integrable models with a narrow bandwidth, not necessarily need the Coulomb potential. Indeed, similar slow dynamics or subdiffusion have been also found in models with dipole-dipole interactions [42], three body interactions [43] and the Bose Hubbard model [44]. It is urgent to demarcate exactly what kind of interactions can lead to slow relaxation in future works.

## Appendix A: initial state for the few spin dynamics

Following [40] and [45], the initial state  $|\psi(0)\rangle$  is created by acting the operator (up to normalization)

$$\sum_x \exp\left(-\frac{(x-x_0)^2}{2\sigma^2}\right) \exp(i(x-x_0)k_0) c_x^\dagger \quad (\text{A1})$$

on an all spin-down state but with  $n$  flipped spins in the center. This operator creates a right going Gaussian wave packet with momentum  $k_0 = -\pi/2$ , width  $\sigma = 4$ , and center position  $x_0$  as depicted in the figure. The dynamics of the collision process is obtained by evolving  $|\psi(0)\rangle$  using TDVP.

## REFERENCES

---

[1] B. Bertini, M. Collura, J. De Nardis, and M. Fagotti, Phys. Rev. Lett. **117**, 207201 (2016).

[2] O. A. Castro-Alvaredo, B. Doyon, and T. Yoshimura, Phys. Rev. X **6**, 041065 (2016).

[3] B. Bertini, F. Heidrich-Meisner, C. Karrasch, T. Prosen, R. Steinigeweg, and M. Žnidarič, Rev. Mod. Phys. **93**, 025003 (2021).

[4] E. Ilievski and J. De Nardis, Phys. Rev. Lett. **119**, 020602 (2017).

[5] J. De Nardis, D. Bernard, and B. Doyon, SciPost Phys. **6**, 049 (2019).

[6] M. Ljubotina, M. Žnidarič, and T. Prosen, Phys. Rev. Lett. **122**, 210602 (2019).

[7] S. Gopalakrishnan and R. Vasseur, Phys. Rev. Lett. **122**, 127202 (2019).

[8] A. J. Friedman, S. Gopalakrishnan, and R. Vasseur, Phys. Rev. B **101**, 180302(R) (2020).

[9] A. Bastianello, A. D. Luca, and R. Vasseur, J. Stat. Mech.: Theory Exp. **2021** (11), 114003.

[10] S. Langer, F. Heidrich-Meisner, J. Gemmer, I. P. McCulloch, and U. Schollwöck, Phys. Rev. B **79**, 214409 (2009).

[11] V. B. Bulchandani, C. Karrasch, and J. E. Moore, PNAS **117**, 12713 (2020).

[12] X. Zotos, Phys. Rev. Lett. **92**, 067202 (2004).

[13] P. Jung, R. W. Helmes, and A. Rosch, Phys. Rev. Lett. **96**, 067202 (2006).

[14] Y. Kagan and L. A. Maksimov, J. Exp. Theor. Phys. **60**, 201 (1984).

[15] W. De Roeck and F. Huveneers, Commun. Math. Phys. **332**, 1017 (2014).

[16] T. Grover and M. P. A. Fisher, J. Stat. Mech. **2014**, P10010 (2014).

[17] M. Schiulaz and M. Müller, AIP Conf. Proc. **1610**, 11 (2014).

[18] M. Schiulaz, A. Silva, and M. Müller, Phys. Rev. B **91**, 184202 (2015).

[19] N. Yao, C. Laumann, J. Cirac, M. Lukin, and J. Moore, Phys. Rev. Lett. **117**, 240601 (2016).

[20] A. A. Michailidis, M. Žnidarič, M. Medvedyeva, D. A. Abanin, T. Prosen, and Z. Papić, Phys. Rev. B **97**, 104307 (2018).

[21] K. Baumann, C. Guerlin, F. Brennecke, and T. Esslinger, Nature **464**, 1301 (2010).

[22] R. Landig, L. Hraby, N. Dogra, M. Landini, R. Mottl, T. Donner, and T. Esslinger, Nature **532**, 476 (2016).

[23] Z. Papic, E. M. Stoudenmire, and D. A. Abanin, Ann Phys-new York **362**, 714 (2015).

[24] S. Capponi, D. Poilblanc, and T. Giamarchi, Phys. Rev. B **61**, 13410 (2000).

[25] M. Hohenadler, S. Wessel, M. Daghofer, and F. F. Assaad, Phys. Rev. B **85**, 195115 (2012).

[26] Z.-H. Li, J. Phys.: Condens. Matter **31**, 255601 (2019).

[27] J. Ren, W.-L. You, and X. Wang, Phys. Rev. B **101**, 094410 (2020).

[28] M. Ljubotina, M. Žnidarič, and T. Prosen, Nat Commun **8**, 16117 (2017).

[29] J. Haegeman, C. Lubich, I. Oseledets, B. Vandereycken, and F. Verstraete, Phys. Rev. B **94**, 165116 (2016).

[30] G. M. Crosswhite, A. C. Doherty, and G. Vidal, Phys. Rev. B **78**, 035116 (2008).

[31] P. Weinberg and M. Bukov, SciPost Phys. **2**, 003 (2017).

[32] H. Bethe, Z. Physik **71**, 205 (1931).

[33] M. Takahashi, Thermodynamics of One-Dimensional Solvable Models (2005).

[34] A. Wöllert and A. Honecker, Phys. Rev. B **85**, 184433 (2012).

[35] J. Mossel and J.-S. Caux, New J. Phys. **12**, 055028 (2010).

[36] K. Winkler, G. Thalhammer, F. Lang, R. Grimm, J. Hecker Denschlag, A. J. Daley, A. Kantian, H. P. Büchler, and P. Zoller, Nature **441**, 853 (2006).

[37] M. Valiente, Phys. Rev. A **81**, 042102 (2010).

[38] D. C. Mattis, Rev. Mod. Phys. **58**, 361 (1986).

[39] P. E. Kornilovitch, EPL **103**, 27005 (2013), publisher: IOP Publishing.

[40] M. Ganahl, M. Haque, and H. G. Evertz, arXiv preprint arXiv:1302.2667 (2013).

[41] R. Vlijm, M. Ganahl, D. Fioretto, M. Brockmann, M. Haque, H. G. Evertz, and J.-S. Caux, Phys. Rev. B **92**, 214427 (2015).

[42] L. Barbiero, C. Menotti, A. Recati, and L. Santos, Phys. Rev. B **92**, 180406(R) (2015).

[43] S. E. Spielman, A. Handian, N. P. Inman, T. J. Carroll, and M. W. Noel, Slow Thermalization of Few-Body Dipole-Dipole Interactions (2022), arXiv:2208.02909 [quant-ph].

[44] A. Bols and W. De Roeck, J. Math. Phys. **59**, 021901 (2018), publisher: American Institute of Physics.

[45] T. Ulbricht and P. Schmitteckert, EPL **86**, 57006 (2009).